Malate-dependent Fe accumulation is a critical checkpoint in the root developmental response to low phosphate

Javier Mora-Macías[a,1], Jonathan Odilón Ojeda-Rivera[a,1], Dolores Gutiérrez-Alanís[a], Lenin Yong-Villalobos[a], Araceli Oropeza-Aburto[a], Javier Raya-González[a], Gabriel Jiménez-Domínguez[a], Gabriela Chávez-Calvillo[a], Rubén Rellán-Álvarez[a], and Luis Herrera-Estrella[a,2]

[a]Laboratorio Nacional de Genómica para la Biodiversidad/Unidad de Genómica Avanzada, Centro de Investigación y Estudios Avanzados, Instituto Politécnico Nacional, 36821 Irapuato, Guanajuato, México

Contributed by Luis Herrera-Estrella, March 10, 2017 (sent for review February 8, 2017; reviewed by Leon V. Kochian and Kashchandra G. Raghothama)

Low phosphate (Pi) availability constrains plant development and seed production in both natural and agricultural ecosystems. When Pi is scarce, modifications of root system architecture (RSA) enhance the soil exploration ability of the plant and lead to an increase in Pi uptake. In *Arabidopsis*, an iron-dependent mechanism reprograms primary root growth in response to low Pi availability. This program is activated upon contact of the root tip with low-Pi media and induces premature cell differentiation and the arrest of mitotic activity in the root apical meristem, resulting in a short-root phenotype. However, the mechanisms that regulate the primary root response to Pi-limiting conditions remain largely unknown. Here we report on the isolation and characterization of two low-Pi insensitive mutants (*lpi5* and *lpi6*), which have a long-root phenotype when grown in low-Pi media. Cellular, genomic, and transcriptomic analysis of low-Pi insensitive mutants revealed that the genes previously shown to underlie *Arabidopsis* Al tolerance via root malate exudation, known as SENSITIVE TO PROTON RHIZOTOXICITY (*STOP1*) and ALUMINUM ACTIVATED MALATE TRANSPORTER 1 (*ALMT1*), represent a critical checkpoint in the root developmental response to Pi starvation in *Arabidopsis thaliana*. Our results also show that exogenous malate can rescue the long-root phenotype of *lpi5* and *lpi6*. Malate exudation is required for the accumulation of Fe in the apoplast of meristematic cells, triggering the differentiation of meristematic cells in response to Pi deprivation.

phosphate | root response | iron | cell differentiation | gene regulation

Phosphorus is an essential nutrient for plant development, a constituent of key molecules such as nucleic acids, ATP, and membrane phospholipids. Plants take up and metabolize phosphorus in the inorganic form of orthophosphate (Pi) (1). Pi is the least accessible macronutrient in many natural and agricultural ecosystems and its low availability in the soil often limits plant growth and productivity. Under phosphate-limiting conditions (−Pi), plants activate an array of genetic (2–6), biochemical (7, 8), and morphological modifications (9–11) that enhance their ability to cope with low Pi availability.

Arabidopsis responses to low Pi availability have been divided in systemic responses that depend upon the internal Pi status of the plant and local responses that depend upon the level of Pi available in the external medium (5, 12). A molecular dissection of local and systemic responses to Pi starvation using transcriptomic analysis has been reported (5). Systemic responses include the up-regulation of genes involved in the overall enhancement of Pi uptake and Pi internal use efficiency and are largely controlled by the master regulator PHR1 (a Myb transcription factor) (6, 13). Local responses include alterations of root traits such as the inhibition of primary root growth (14), an increase in lateral root density (10), and higher density and length of root hairs (9). These changes in root system architecture (RSA) have been proposed to enhance the soil exploration ability of the plant by increasing root surface area of exploration in the top layers of the soil where Pi tends to accumulate. Some evidence indicates that there is some degree of cross-talk between local and systemic responses to low Pi availability, as mutants altered in RSA responses to low Pi also have an altered expression of genes involved in systemic responses (15).

Growth of *Arabidopsis* seedlings under in vitro Pi-limiting conditions induces a determinate developmental program known as root apical meristem (RAM) exhaustion (11). RAM exhaustion consists of the loss of meristematic potential and the arrest of cell proliferation, leading to the inhibition of primary root growth. Meristematic potential is lost due to premature differentiation of the cells that constitute the stem cell niche (SCN), which includes the quiescent center (QC). Cell proliferation in the RAM is lost due to a gradual reduction in mitotic activity. Root-tip contact with low phosphate media (16) in the presence of iron (17) has been reported as essential for the inhibition of primary root growth in response to Pi-deficiency conditions in *Arabidopsis thaliana*. *Arabidopsis* mutants that fail to trigger root system morphological responses to low Pi have been reported previously

Significance

Phosphate (Pi) deficiency constrains plant development and productivity in both natural and agricultural ecosystems. An interaction among Pi and Fe availability controls the developmental program that allows the *Arabidopsis* root system to more effectively explore the topsoil where Pi accumulates. Analysis of mutants unable to establish root architecture responses to low Pi allowed the identification of mutant alleles of *STOP1* (a transcription factor) and *ALMT1* (a malate transporter), two genes previously reported to play a role in the malate-mediated tolerance to toxic levels of aluminum. We show that these genes underlie a malate-exudation–dependent mechanism of Fe relocation in the root apical meristem that is essential for reprogramming root growth under low-Pi conditions.

Author contributions: J.M.-M., J.O.O.-R., L.Y.-V., R.R.-Á., and L.H.-E. designed research; J.M.-M., J.O.O.-R., D.G.-A., L.Y.-V., A.O.-A., J.R.-G., G.J.-D., and G.C.-C. performed research; L.H.-E. contributed new reagents/analytic tools; J.M.-M., J.O.O.-R., L.Y.-V., J.R.-G., G.J.-D., R.R.-Á., and L.H.-E. analyzed data; and J.M.-M., J.O.O.-R., R.R.-Á., and L.H.-E. wrote the paper.

Reviewers: L.V.K., University of Saskatchewan; and K.G.R., Purdue University.

Conflict of interest statement: L.H.-E. and Leon V. Kochian were coauthors on a 2013 publication. This publication was a review article and did not involve any research collaboration.

Freely available online through the PNAS open access option.

Data deposition: The data reported in this paper have been deposited in the Gene Expression Omnibus (GEO) database, www.ncbi.nlm.nih.gov/geo (accession no. GSE90061) and at National Center for Biotechnology Information Biosample database www.ncbi.nlm.nih.gov/biosample/ (accession nos. SAMN06013467; SAMN06013468; SAMN06013469; SAMN06013470).

[1]J.M.-M. and J.O.O.-R. contributed equally to this work.

[2]To whom correspondence should be addressed. Email: lherreae@cinvestav.mx.

This article contains supporting information online at www.pnas.org/lookup/suppl/doi:10.1073/pnas.1701952114/-/DCSupplemental.

(15, 16). Two of these mutants, low phosphate root 1 and 2 (*lpr1 and lpr2*) were found to be affected in genes encoding multicopper oxidases, suggesting that a metal with different levels of oxidation could be involved in the alteration of root system architecture in response to low Pi availability (16). A mutant that is hypersensitive to low Pi, phosphate deficiency response 2 (*pdr2*), and triggers the root system response to low Pi availability faster that the wild type (WT) was also reported (18). *PDR2* encodes an endoplasmic reticulum (ER)-localized P_5-type ATPase (19). *PDR2* and *LPR1* have been proposed to orchestrate RAM exhaustion in a genetically interacting route under low-Pi conditions (19). Whereas the precise function of PDR2 has not been determined, LPR1 is essential for primary root inhibition under low-Pi conditions and it has been shown to have ferroxidase activity (16, 19, 20). An LPR1-dependent accumulation of Fe^{+3} in the apoplast of cells in the elongation and meristematic regions of the primary root, that triggers the production of reactive oxygen species (ROS), is essential for meristem exhaustion in low-Pi media (20). ROS generation correlates with callose deposition in the RAM, which was proposed to activate meristem exhaustion by blocking the cell-to-cell movement of SHORT-ROOT (SHR), a transcription factor that is essential for stem cell maintenance in the RAM (20). However, the mechanism that regulates iron accumulation and relocation in the RAM remains largely unknown.

In this work, we characterized two **l**ow **p**hosphate **i**nsensitive mutants (*lpi5 and lpi6*), which, in contrast to the short-root phenotype of WT *Arabidopsis* seedlings, show normal primary root elongation in low-Pi media. Mapping by sequencing revealed that the *lpi5* corresponds to SENSITIVE TO PROTON RHIZOTOXICITY (*STOP1*) and *lpi6* to ALUMINUM ACTIVATED MALATE TRANSPORTER 1 (*ALMT1*), the two genes previously reported to be responsible for activating malate efflux in the roots of *Arabidopsis* seedlings exposed to toxic concentrations of aluminum (21–23). Genetic, cellular, and transcriptomic analyses show that *STOP1* and *ALMT1* are required for a malate-dependent accumulation of iron in the root meristem, which leads to alterations in the redox balance that trigger primary root growth inhibition and RAM exhaustion in response to Pi-deficiency conditions in *A. thaliana*.

Results

***Arabidopsis* EMS Mutants *lpi5* and *lpi6* Show Indeterminate Primary Root Growth Under Phosphate-Deficiency Conditions.** The *A. thaliana* Col-0 accession seedlings grown in media containing low-Pi concentrations (below 50 μM Pi) show a short-root phenotype defined by a determinate pattern of primary root growth and RAM differentiation. To identify mutants that are insensitive to the effect of low Pi on primary root growth, we screened an EMS-mutagenized Col-0 population for mutant lines presenting a long-root phenotype under low-Pi (−Pi, 5 μM Pi) conditions. We isolated ∼50 mutant lines with different alterations in the primary root growth in response to low Pi availability. Two lines that were insensitive to the effect of low Pi on primary root growth, which we named low phosphorus insensitive 5 and low phosphorus insensitive 6 (*lpi5* and *lpi6*), were chosen for further characterization (Fig. 1 *A*–*C*). When grown under high Pi (+Pi; 1,000 μM Pi) conditions, both *lpi5* and *lpi6* seedlings presented a primary root length similar to the WT *Arabidopsis* Col-0 accession (Fig. 1 *A* and *C*). Under −Pi conditions at 10 d after germination (dag), WT plants had a visible reduction in primary root growth, whereas *lpi5* and *lpi6* seedlings had primary root elongation similar to that of WT seedlings grown in +Pi media, which is fourfold longer than that of Pi-deprived WT seedlings (Fig. 1 *A* and *C*). Although *lpi5* seedlings had a long-root phenotype in −Pi media, they had a slightly shorter primary root than the WT and *lpi6* in +Pi media and were also slightly shorter than *lpi6* in −Pi medium (Fig. 1 *A* and *C*). Analysis of segregation frequencies under −Pi conditions showed that the long-root phenotype in *lpi5 and lpi6* is the result of single recessive mutations (*SI Appendix*, Table S1).

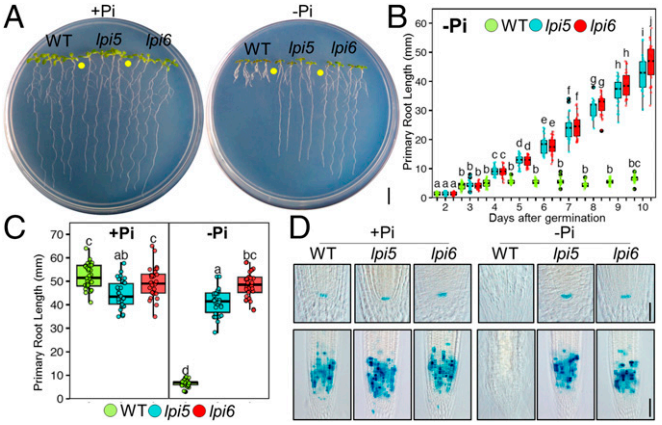

Fig. 1. Low-Pi insensitive mutants continue primary root growth and RAM maintenance under Pi-deficiency conditions. (*A*) Phenotypes of WT, *lpi5*, and *lpi6* seedlings grown under high (1,000 μM Pi; +Pi)- and low-Pi (5 μM Pi; −Pi) conditions 10 dag. (Scale bar, 1 cm.) (*B*) Primary root growth kinetics of seedlings grown under −Pi conditions from 2 to 10 dag. Green, blue, and red dots depict WT, *lpi5*, and *lpi6* individuals (n = 30 from three independent experiments), respectively. Statistical groups were determined using a Tukey honest significant difference (HSD) test (P value <0.05) and are indicated with letters. (*C*) Primary root length of seedlings grown under +Pi and −Pi conditions. Green, blue, and red dots depict WT, lpi5, and lpi6 individuals (n = 30 from three independent experiments), respectively. Statistical groups were determined using a Tukey HSD test (P value <0.05) and are indicated with letters. (*D*) GUS staining of *proCycB1::GUS* and *proQC46::GUS* expression in the RAM of WT, *lpi5*, and *lpi6* seedlings 10 dag. (Scale bar, 100 μm.)

In Pi-deprived *Arabidopsis* seedlings, the short-root phenotype is accompanied by a reduction in cell proliferation and meristematic activity during the process of RAM exhaustion (11). To test for signs of RAM exhaustion in *lpi5* and *lpi6* seedlings grown in −Pi media, we examined the expression of the *proCycB1::GUS* cell cycle activity marker (24) and the *proQC46::GUS* QC identity marker (25). In +Pi media, WT, *lpi5*, and *lpi6* seedlings showed clear cell proliferation activity as indicated by the *proCycB1::GUS* signal and an active QC as shown by the *proQC46::GUS* signal (Fig. 1*D*). In −Pi media at 10 dag, the cell cycle and QC marker genes were undetectable in WT seedlings, whereas GUS staining was clearly detectable for both the cell cycle (*proCycB1::GUS*) and QC (*proQC46::GUS*) markers in the primary root of *lpi5* and *lpi6* (Fig. 1*D*). These results show that, in contrast to the WT, low Pi does not trigger meristem exhaustion in the RAM of *lpi5* and *lpi6* seedlings.

***lpi5* and *lpi6* Have Mutations in the Transcription Factor *STOP1* and the Malate Transporter *ALMT1*, Respectively.** We used a mapping-by-sequencing approach to identify the genes responsible for the *lpi5* and *lpi6* phenotypes (*Materials and Methods*). We identified 12 and 18 specific homozygous variants (missense, frameshift, and splice donor) potentially linked to *lpi5* and *lpi6* mutant phenotypes, respectively. Given the alterations of primary root of *lpi5* and *lpi6* seedlings in response to an environmental stress, we focused on the homozygous mutations that could potentially be linked to alterations in root morphology or root responses to abiotic stress. Among the potential candidates responsible for the root phenotype of *lpi5* and *lpi6* under low-Pi conditions, SENSITIVE TO PROTON RHIZOTOXICITY (*STOP1*) and ALUMINUM ACTIVATED MALATE TRANSPORTER 1 (*ALMT1*) were particularly interesting because both genes have been previously reported to participate in the tolerance of the *Arabidopsis* root to toxic concentrations of Al^{+3}. *STOP1* (*At1g34370*) encodes a zinc finger protein transcription factor that plays a critical role in Al^{+3} tolerance and acid soil tolerance in *Arabidopsis* (21). *ALMT1* encodes a transmembrane protein that mediates malate efflux in the

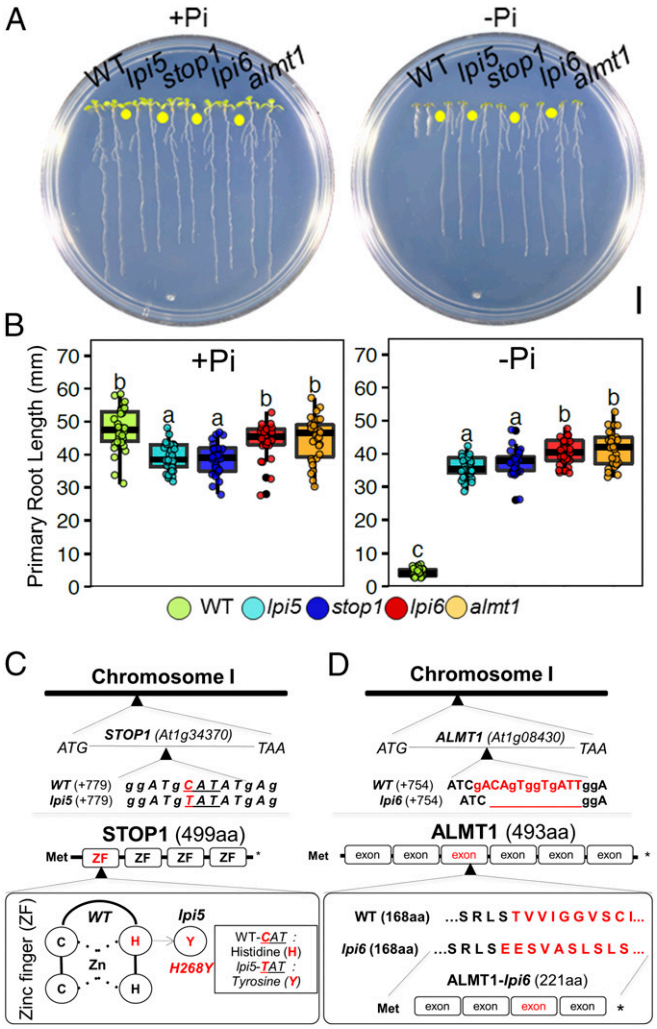

Fig. 2. Mapping by sequencing revealed *lpi5 and lpi6* to be *stop1* and *almt1* mutants, respectively. (*A*) Phenotypes of Col-0, *lpi5*, *stop1*, *almt1*, and *lpi6* seedlings grown under high-phosphate (+Pi) and low-phosphate (−Pi) conditions 10 dag. (Scale bar, 1 cm.) (*B*) Primary root length of WT, *lpi5*, *stop1*, *almt1*, and *lpi6* seedlings grown under high-phosphate (+Pi) or low-phosphate (−Pi) conditions 10 dag. Dots depict WT, *lpi5*, *stop1*, *almt1*, and *lpi6* individuals (n = 30 from three independent experiments). Statistical groups were determined using a Tukey HSD test (P value <0.05) and are indicated with letters. (*C*) C:T (CAT: TAT) substitution in the +84 base within the At1g34370 locus of the *lpi5* genome. *lpi5* mutation causes an amino acid substitution (H168Y) that replaces one of the two histidine residues of the four zinc fingers that constitute STOP1. (*D*) A 13-bp deletion in the +757 base pair position within the first exon of the At1g08430 locus of the *lpi6* genome. The 13-bp deletion present in *lpi6* causes a frameshift mutation that produces an aberrant protein with 200 amino acids less than the WT. Met, methionine.

root in response to the presence of toxic Al^{+3} levels (22), and its expression has been shown to be activated by *STOP1* in response to Al stress conditions (21).

To test whether the long-root phenotype of *lpi5* and *lpi6* was indeed due to lesions in STOP1 and ALMT1, we tested the phenotype of T-DNA insertional mutants in *STOP1* (*SALK_114108*) and *ALMT1* (*SALK_009629*) in −Pi and +Pi media. In +Pi media, WT, *lpi6*, and *almt1* seedlings had a similar primary root length, whereas *lpi5* and *stop1* had a slightly shorter root length than the WT (Fig. 2 *A* and *B*). In −Pi media, the T-DNA insertional mutants *stop1* and *almt1* had a long-root phenotype that contrasted with the short-root phenotype of the WT (Fig. 2 *A* and *B*). It has been reported that *stop1* is sensitive to low pH (4.7) and levels of Al^{+3} (2 μM) that are not yet toxic for *Arabidopsis* WT seedlings and that *almt1* is also sensitive to this Al^{+3} concentration (26). We also found that *lpi5* was sensitive to low pH and Al (as is *stop1*) and that *lpi6* was sensitive to Al but not to low pH (as observed for *almt1*) (*SI Appendix*, Fig. S1). Crosses between *lpi5* and *almt1* and between *lpi6* and *stop1* showed that *lpi5* and *lpi6* are mutant alleles of *STOP1* and *ALMT1*, respectively (*SI Appendix*, Fig. S1).

Mapping by sequencing of *lpi5* revealed a C:T (CAT:TAT) substitution in the +84 position of *STOP1*. In silico analysis predicted that the *lpi5* mutation caused an amino acid substitution (H168Y) that replaces one of the two histidine residues that are crucial for the formation of the first of four zinc fingers of the DNA binding domain of STOP1 (Fig. 2*C*). The first zinc finger domain of STOP1 is critical to bind to the promoter of its target genes (27). Mapping by sequencing of the *lpi6* mutant revealed a 13-base pair deletion in the first exon of *ALMT1* starting at position +757 (Fig. 2*D*). In silico analysis predicted that this deletion causes a frameshift mutation that produces an aberrant protein that lacks 221 amino acids of the carboxyl-terminal moiety of ALMT1 (Fig. 2*D*). Our in silico sequence analysis further confirmed that *lpi5* and *lpi6* are EMS-induced mutant alleles of *STOP1* and *ALMT1*, respectively.

***ALMT1* Is Expressed in the RAM of *Arabidopsis* Under Pi-Deficiency Conditions Before Meristematic Exhaustion.** To determine whether the expression of *STOP1* and *ALMT1* is regulated by Pi availability in the root tip, we analyzed the expression of *STOP1* and *ALMT1* in the root apex of 5 dag WT and *stop1* seedlings using qRT-PCR (Fig. 3*A* and *SI Appendix*, Fig. S3). In the WT, *ALMT1* expression increased by approximately fourfold in response to −Pi conditions, whereas the level of expression of *STOP1* was not significantly altered by Pi availability (Fig. 3*A*). We also found that in the *stop1* background, the expression of *ALMT1* was undetectable (*SI Appendix*, Fig. S2). Our results confirm a previous report (21) showing that *STOP1* is essential

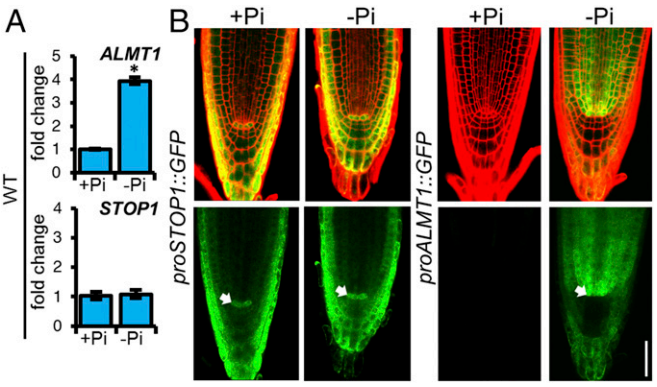

Fig. 3. *STOP1* and *ALMT1* are expressed in the RAM of *Arabidopsis* under Pi-deficiency conditions. (*A*) qRT-PCR analysis of *STOP1* and *ALMT1* expression in the root apex (2–3 mm) of WT (Col-0) plants. Bars represent the mean fold change ± SEM of two biological replicates with three technical replicates. WT +Pi samples were used as calibrator values. *ACT2* and *UBQ10* were used as internal controls. Asterisk indicates that the expression was significantly different between +Pi and −Pi conditions (Student t test; *P < 0.05). (*B*) Transgenic Col-0 plants harboring transcriptional gene fusions containing the *STOP1* and *ALMT1* promoter fused to a double GFP–GUS reporter gene, respectively (*proSTOP1::GUS::GFP* and *proALMT1::GUS::GFP*), were grown under +Pi and −Pi conditions and expression activity was observed at 5 dag using confocal microscopy. (*Upper*) Merged propidium iodine staining fluorescence (red) and GFP fluorescence (green). (*Lower*) GFP fluorescence. Arrow points to the stem cell niche region. (Scale bar, 100 μm.)

for the expression of *ALMT1*, but also show that *STOP1* is required for the induction of *ALMT1* in response to low Pi.

Because *STOP1* and *ALMT1* appear to be essential for RAM exhaustion under Pi-deficiency conditions, we examined the cell-specific expression pattern of these two genes in seedlings grown under +Pi and −Pi conditions 5 dag, a time point before full RAM exhaustion (Fig. 1*C*), but when primary root growth inhibition has already started (Fig. 1*C*). Confocal microscopy of *proSTOP1::GUS::GFP* seedlings grown in +Pi media revealed that *STOP1* is expressed in the QC, columella, lateral root cap, and epidermis (Fig. 3*B*) and that its expression pattern is not altered in −Pi media (Fig. 3*B*). On the other hand, no detectable reporter activity of *proALMT1::GUS::GFP* was found in the RAM of seedlings grown under +Pi conditions, whereas in −Pi media expression of the reporter gene was clearly detectable in the proximal region of the SCN (QC, cortex, and stele initials), vascular bundle, pericycle, cortex, endodermis, columella, and lateral root cap (Fig. 3*B*).

Malate Treatment Rescues the Determinate Developmental Program in the Primary Root of *stop1* and *almt1* in Response to Low-Pi Conditions. Because malate efflux has been shown to be affected in *stop1* and *almt1* mutants and both *stop1* and *almt1* present determinate primary root growth under Al^{+3} toxicity conditions (21, 22), we sought to determine whether malate exudation also played a role in the *Arabidopsis* primary root response to low Pi availability. To this end, we added increasing concentrations of malate to both +Pi and −Pi media and tested the effect of malate treatment on the primary root growth of WT, *stop1*, and *almt1* seedlings (Fig. 4 and *SI Appendix*, Fig. S3). We observed that primary root growth was not altered by malate treatment under +Pi conditions in any of the tested lines (*SI Appendix*, Fig. S3). However, in −Pi media, treatment with malate restored the short-root phenotype in *stop1* and *almt1* seedlings in a concentration-dependent manner (Fig. 4 *A* and *B*). Although *stop1* seedlings treated with 1 mM malate had significantly shorter roots than in media lacking malate, their primary roots were slightly, but statistically significantly, larger than those of the WT and *almt1* seedlings grown in the same media (Fig. 4 *A* and *B*). Malate treatment of Pi-deprived WT seedlings showed a small effect at 0.1 mM; however, this effect was not observed at higher malate concentrations (Fig. 4 *A* and *B*) as WT seedlings remained short under all treatments (Fig. 4*A*).

To determine whether malate treatment activates RAM exhaustion in *stop1* and *almt1* seedlings, we examined the expression of *proCycB1::GUS* and *proQC46::GUS* reporter genes in Pi-deprived/malate-treated *stop1* and *almt1* seedlings. Clear signs of cell differentiation in the RAM of Pi-deprived/malate-treated *almt1* seedlings were observed and *proCycB1::GUS* and *proQC46::GUS* reporter activity was undetectable. In the case of Pi-deprived/malate-treated *stop1* seedlings, although cell proliferation was reduced, it was not completely arrested and *proQC46::GUS* expression was still clearly detectable (Fig. 4*C*). No expression was found in the WT either in low-Pi media or low-Pi media supplemented with 1 mM malate (Fig. 4*C*).

Fe Accumulation Is Absent in the RAM of Pi-Deprived *stop1* and *almt1* Seedlings and Can Be Rescued by Malate Treatment. Accumulation of Fe in the apoplast of cells in the RAM is required to activate the primary root response to low Pi availability (20). As carboxylate–iron complexes have been reported to participate in iron transport and acquisition in plants (28–30) and malate efflux is affected in *stop1* and *almt1* mutants (21, 22), we explored whether malate exudation plays a role in the Fe accumulation mechanism that is required to trigger primary root growth inhibition in response to low Pi availability. First, we tested whether malate is required for the accumulation of Fe in the apoplast of RAM cells using Perls-diaminobenzidine (DAB) histochemical Fe staining, which allows the detection of changes in labile Fe^{+3} (20), on the root tips of WT, *stop1*, and *almt1* in low-Pi media with or without 1 mM malate (Fig. 4*D* and *SI Appendix*, Fig. S3). In Pi-deprived seedlings not exposed to malate, Fe staining was clearly observed in the roots of WT seedlings, whereas *stop1* and *almt1* seedlings showed a much lower Fe accumulation (Fig. 4*D*). In Pi-deprived WT seedlings treated with 1 mM malate, Fe staining was still clearly

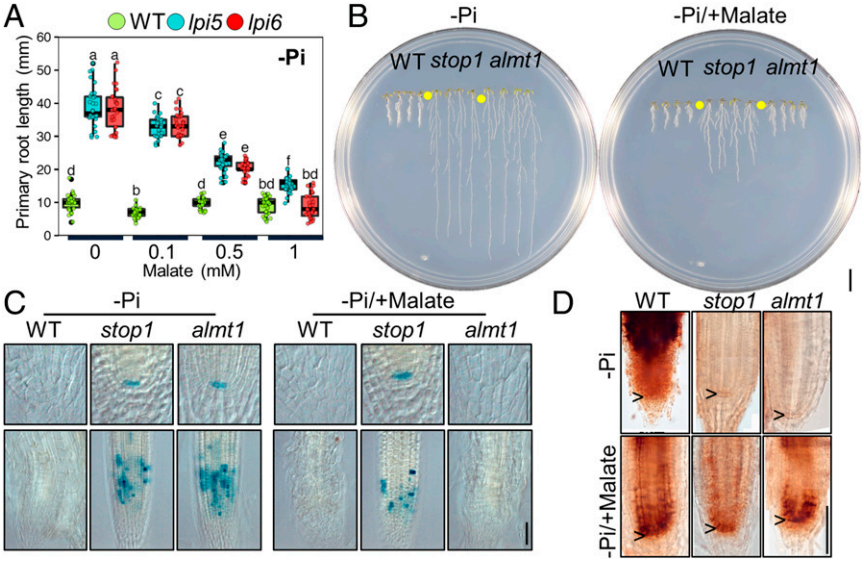

Fig. 4. Malate treatment rescues the mutant phenotype of *stop1* and *almt1* seedlings. (*A*) Primary root length of 10 dag WT, *stop1*, and *almt1* seedlings grown under increasing concentration of malate supplemented into −Pi medium. Green, blue, and red dots depict WT, *stop1*, and *almt1* individuals ($n = 30$ from three independent experiments), respectively. Statistical groups were determined using Tukey HSD test (P value <0.05) and are indicated with letters. (*B*) Phenotypes of 10 dag WT, *stop1*, and *almt1* seedlings grown under low-phosphate medium (−Pi) and low-phosphate medium supplemented with 1 mM malate (−Pi/+malate). (Scale bar, 1 mm.) (*C*) *proCycB1::GUS* (*Lower*) and *proQC46::GUS* (*Upper*) expression. (*D*) Perls-DAB iron staining in the RAM of WT, *stop1*, and *almt1* seedlings grown under −Pi and malate treatment (1 mM; −Pi/+malate) conditions 5 dag. Pictures show photographic reconstructions in which several images were spliced together to show the complete primary root meristem (*Materials and Methods*). (Scale bar, 50 μm.)

visible but in a more defined zone of the root apex, which included the QC. In contrast to *stop1* and *almt1* seedlings grown in −Pi media lacking malate, those treated with 1 mM of this organic acid showed a very similar pattern to that observed for the WT under the same conditions. Although malate-treated Pi-deprived *stop1* seedlings show a clear Fe staining, accumulation of Fe^{+3} in the RAM was apparently lower around the QC than that observed for the WT and *almt1* seedlings treated with malate (Fig. 4*C*). We did not observe significant differences in the patterns of Fe staining between the root tips of WT, *stop1*, and *almt1* seedlings under +Pi conditions treated with 1 mM malate (*SI Appendix*, Fig. S3).

Citrate, as well as malate, is an organic acid that is released by plant roots in response to low Pi availability (31). Because organic acids are naturally occurring metal chelating agents, and if the malate chelating effect is responsible for the primary root growth inhibition in −Pi media, we wanted to test whether citrate treatment of Pi-deprived seedlings (1 mM citrate) could also phenocopy the short-root phenotype in Pi-deprived *stop1* and *almt1* seedlings. In −Pi media, we observed that citrate treatment slightly reduced primary root elongation of *stop1* seedlings (10%) (*SI Appendix*, Fig. S4 *A* and *B*) and had no significant effect in the root growth of Pi-deprived *almt1* seedlings (*SI Appendix*, Fig. S4 *A* and *B*). Interestingly, citrate treatment of Pi-deprived WT seedlings resulted in an average 2.5-fold increase in root length compared with that observed for WT seedlings grown in low-Pi media in the absence of citrate (*SI Appendix*, Fig. S4 *A* and *B*). These results suggest a specific role of malate in primary root growth inhibition by promoting the accumulation of Fe in the apoplast of root cells in the meristematic area.

As malate is capable of inducing root growth inhibition and meristem exhaustion in *almt1* seedlings, linked to an effect on Fe accumulation in the RAM of *almt1* seedlings, we hypothesized that malate has a chelating effect on Fe that contributes to its accumulation in the root tip. To test our hypothesis, we performed molecular dynamic calculations to simulate the effect of malate on the aggregation of metallic ions such as Fe^{+2}, Fe^{+3}, and Al^{+3}. We built four different simulation sets using ascending malate:metal molecular ratios: 0:120–120:120 (*SI Appendix*, Fig. S5). We observed nonbonded interactions between malate and Fe^{+2} ions but the interactions did not induce Fe^{+2} aggregation in any of the simulated systems (*SI Appendix*, Fig. S5). In the case of the malate and Fe^{+3} system we observed nonbonded interactions and the formation of large malate–Fe^{+3} aggregates in all ratios tested with an increasing size of aggregates when an equimolar concentration of malate and Fe^{+3} was used (*SI Appendix*, Fig. S5). Metals did not aggregate when malate was not included in the simulation set (*SI*

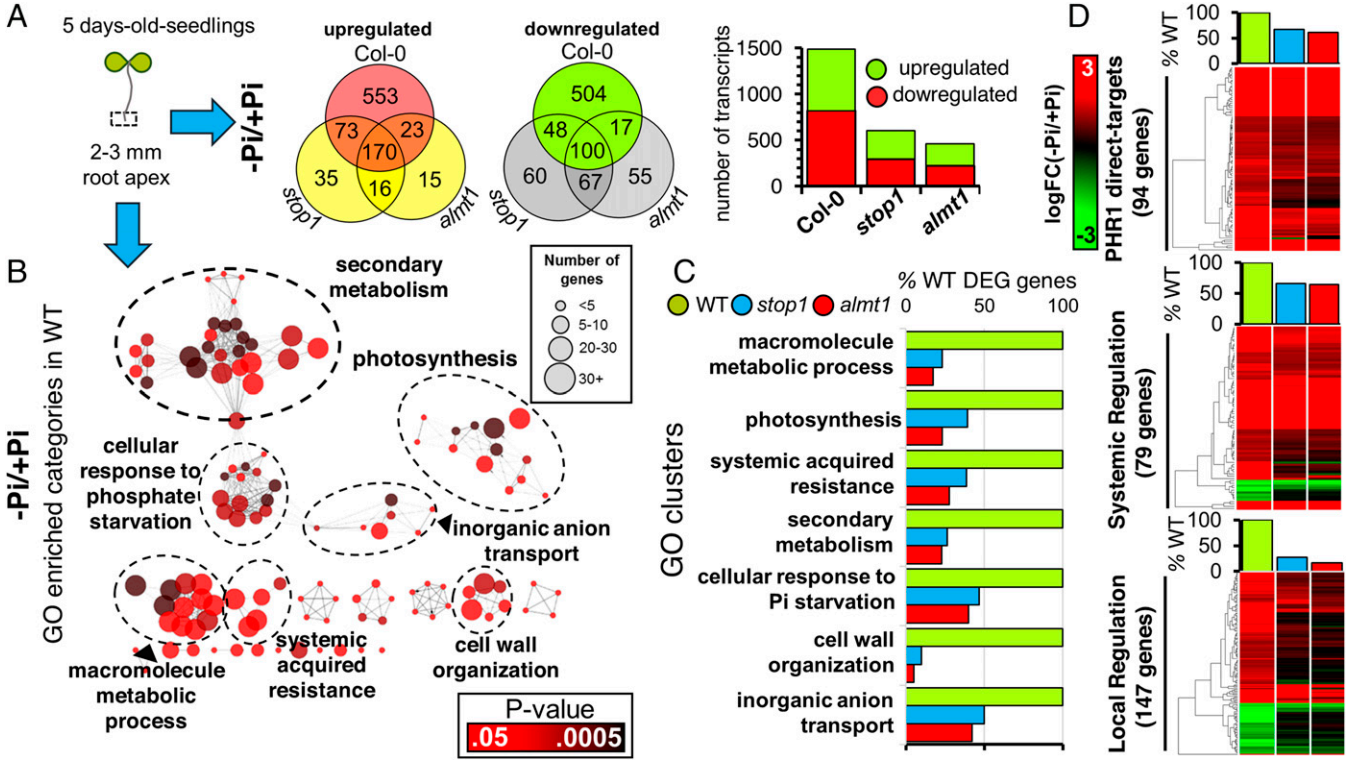

Fig. 5. Differential expression profiling of WT, *stop1*, and *almt1* revealed a loss of transcriptional response to Pi starvation in the root apex of *stop1* and *almt1*. (*A*) Venn diagram of differentially expressed genes (DEG) that are up- and down-regulated [−1.5 > logFC(−Pi/Pi) > 1.5; FDR < 0.05] in the root tip of WT, *stop1*, and *almt1* seedlings in response to −Pi conditions. A bar graph illustrating the number of up-regulated and down-regulated transcripts in WT, *stop1*, and *almt1* is presented. (*B*) Gene ontology (GO) enrichment analysis of overrepresented categories that are activated in the root apex of Pi-deprived WT seedlings. Each circle corresponds to a significantly enriched GO category (*P* value <0.05; hypergeometric test; Benjamini–Hochberg correction). Color code resembles *P* value and size resembles the number of genes that are associated with that respective GO category. GO categories that share genes are connected and clustered by the biological process that corresponds to the most significantly enriched category of the cluster. (*C*) Analysis of DEG by cluster in the root tip of *stop1* and *almt1*. The number of genes that belong to each GO cluster, and are differentially expressed in *stop1* and *almt1*, is presented as a percentage of the number of genes that are differentially expressed in WT (% DEG of WT). (*D*) Transcriptomic analysis of locally and systemically regulated genes in the root apex of WT, *stop1*, and *almt1* revealed a key role of *STOP1* and *ALMT1* in the local response to Pi starvation in *Arabidopsis*. WT, *stop1*, and *almt1* logFC values of genes that are differentially expressed in the root tips of WT seedlings [−1.5 > logFC(−Pi/Pi) > 1.5; FDR < 0.05] in response to −Pi conditions and were reported as PHR1-direct targets (6) and of those that were classified as part of the local or systemic transcriptional response as reported in ref. 5 is represented in a heatmap, respectively. Genes that are differentially expressed in WT root tips and their expression levels in WT, *stop1*, and *almt1* seedlings grown under −Pi conditions are illustrated according to the key.

Appendix, Fig. S5). These results suggest that malate can form large aggregates with Fe^{+3} and Al^{+3} but not with Fe^{+2}, which could be relevant for the activation of the *Arabidopsis* primary root response to low Pi.

Differential Expression Analysis Revealed a Preferential Loss of Local Transcriptional Responses to Pi Starvation in *stop1* and *almt1* Root Tips. The root tip plays a fundamental role in the ability of the root system to sense and respond to Pi starvation (16). Therefore, to understand the role of *STOP1* and *ALMT1* in the local and systemic responses of the *Arabidopsis* root to low phosphate, we performed a whole transcriptome sequencing (RNA-seq) analysis of gene expression in root tips from WT, *stop1*, and *almt1* seedlings grown under +Pi and −Pi conditions (Fig. 5). We performed pairwise comparisons of transcript abundances between −Pi and +Pi conditions to determine differentially expressed genes [−1.5 > logFC > 1.5; false discovery rate (FDR) < 0.05] in response to Pi deficiency in WT, *stop1*, and *almt1* root tips (Fig. 5*A*). A total of 1,488 genes were found to be responsive to low phosphate in the WT (819 up; 669 down), whereas only 569 in *stop1* (294 up; 275 down) and 463 in *almt1* (224 up; 239 down) (Fig. 5*A*). To identify the biological processes whose expression is misregulated in the root apex of *stop1* and *almt1* in response to Pi availability, we performed a gene ontology (GO) enrichment analysis (Fig. 5). First, we performed a GO clusterization of all of the over-represented categories that included genes that belong to the same biological process in the root tips of WT seedlings (Fig. 5*B*). We found seven clusters that were named after the most significantly overrepresented category of the cluster and included the cellular response to phosphate starvation (GO:0016036), secondary metabolism (GO:0019748), macromolecule metabolic process (GO:0044260), cell wall organization (GO:0071555), and systemic acquired resistance (GO:0009627). A full list of the GO categories that were enriched in the WT is included in Dataset S1. We then performed an analysis of the percentage of genes belonging to each cluster that were differentially expressed in *stop1* and *almt1* relative to the WT (Fig. 5*C*). Using such an approach, we determined that, overall, the percentage of genes that were activated in response to low phosphate in the root tip of the WT and misregulated in *stop1* and *almt1* ranged between 40% and 95% (Fig. 5*C*). The most affected biological process was "cell wall organization" as evidenced by the reduced number of transcripts from the cluster that were activated in response to low Pi in *stop1* and *almt1* (41 WT; 4 *stop1*; 2 *almt1*). Of the 46 differentially expressed genes included in the "response to phosphate starvation" that were regulated in WT root tips, 46% and 40% (21 *stop1*; 18 *almt1*) were differentially expressed in the root tips of *stop1* and *almt1*, respectively.

We found that the expression of *SPX1* and *SPX2*, two key genes in the regulation of Pi-responsive genes that are systemically induced (32), were normally induced in the root tips of *stop1* and *almt1* mutants (Dataset S1). Therefore, we examined the transcription levels of genes that are known targets of the PHR1/SPX systemic regulatory node (6). Of the 94 PHR1 direct targets that we found induced in the root tips of WT plants, we found that 60% (63 *stop1*; 57 *almt1*) were also induced in *stop1* and *almt1* in response to low-Pi conditions (Fig. 5*D*). Because the activation of genes in the cell wall organization cluster is one of the most affected in *stop1* and *almt1* and its transcriptional regulation has been recently linked to the local response to low Pi availability (33), our results suggest that the local response to low Pi is largely lost in *stop1* and *almt1* and that the systemic response to low Pi is significantly less affected than the local response in these two mutants. To confirm that this was indeed the case, we performed a comparison of genes that had been previously defined to participate in local and systemic responses to low Pi (5) with those that were not activated in *stop1* and *almt1* (Fig. 5*D*). We found that among the 79 systemic and 147 local genes that were differentially expressed in the WT in response to Pi deficiency under our experimental conditions, over 60% of the systemically regulated genes remained responsive in *stop1* (52 genes) and *almt1* (51 genes), whereas less than 28% of locally regulated genes (40 *stop1*; 24 *almt1*) remained responsive to Pi starvation in the root tips of the mutants (Fig. 5*D*). These results confirm that *STOP1* and *ALMT1* have a key role in regulating the expression of genes in the local response to Pi deficiency. Nonetheless, *STOP1* and *ALMT1* also seem to have a significant effect on a group of genes that are systemically induced by low Pi availability.

Malate Treatment Rescued the Expression of Local-Response Genes Encoding Apoplast-Located Proteins. As we observed that malate treatment rescued iron accumulation in the RAM and the long-root phenotype of *stop1* and *almt1* mutants, we sought to identify the subset of genes that regulate primary root growth inhibition and whose expression under low-Pi conditions is reactivated by malate treatment in *stop1* and *almt1* seedlings. To this end, we isolated mRNA from the root tips of Pi-deprived *stop1* and *almt1* mutants that were treated with malate (1 mM) and carried out RNA-seq analysis (Fig. 6). Our rationale was that the common set of genes that are differentially expressed in the root tips of Pi-deprived seedlings that have a short-root phenotype (WT, *stop1*+M, and *almt1*+M) and that are not differentially expressed (induced or repressed) in the root tips of Pi-deprived *stop1* and *almt1* seedlings, which have a long-root phenotype in −Pi media, are linked to the malate-dependent mechanism that triggers primary root growth inhibition under Pi-deprivation conditions. A common set of 210 differentially expressed genes (63 up-regulated; 147 down-regulated) was found between the genotypes/treatment that induce a short-root phenotype under −Pi conditions and that are not differentially expressed in Pi-deprived seedlings with a long-root phenotype (Fig. 6*A*). Among the genes whose expression was rescued by malate treatment, we found several peroxidase family genes (*PEROXIDASE2*, *PEROXIDASE37*, *AT3G01190*, and *PEROXIDASE4*), which are closely related to the control of ROS homeostasis (34). A full list of the genes and description is included in Dataset S1. Interestingly, using SUBA, a subcellular prediction tool (35), we found that 30% of proteins encoded by genes whose responsiveness to low Pi is restored by malate treatment in *stop1* and *almt1* Pi-deprived seedlings are targeted to the apoplast or extracellular region (Fig. 6*B*), confirming a previous study in which a major role of the apoplast in the root response to Pi starvation was highlighted (33). Furthermore, an additional 16% of genes are targeted to the plasma membrane (Fig. 6*B*).

LPR1 Acts Downstream of STOP1 and ALMT1. In *Arabidopsis*, *LPR1* has been reported to mediate the oxidation of Fe^{+2} to Fe^{+3} in the apoplast, which was correlated with ROS generation that triggers callose deposition in the root apex and disrupts SHR transport, which ultimately induces determinate primary root growth in response to Pi-deficiency conditions (20). As both Fe^{+3} accumulation and the regulation of peroxidases are lost and rescued by malate treatment in *stop1* and *almt1* mutants, using our RNA-seq data, we analyzed whether malate treatment had the same effect on the *LPR1* expression in response to low-Pi conditions in the root apex of *stop1* and *almt1* (Fig. 6*C*). The expression of *LPR1* was found to be enhanced in the root apex of WT seedlings (3.29-fold) exposed to low Pi, induction that was significantly lower in *stop1* (1.64-fold) and *almt1* (1.25-fold) Pi-deprived seedlings (Fig. 6*C*). Our data revealed that, indeed, malate treatment increased *LPR1* transcript levels in Pi-deprived *stop1* seedlings from 1.5- to 2.0-fold and in *almt1* seedlings from 1.2- to 2.7-fold (Fig. 6*C*). The higher increase in *LPR1* expression induced by malate treatment in *almt1* than *stop1* correlates with the capacity of the treatment to better restore the primary root response to low in *almt1* than in *stop1* (Fig. 6*C*). To test whether the effect of malate was dependent or independent of LPR1, we studied the effect of malate

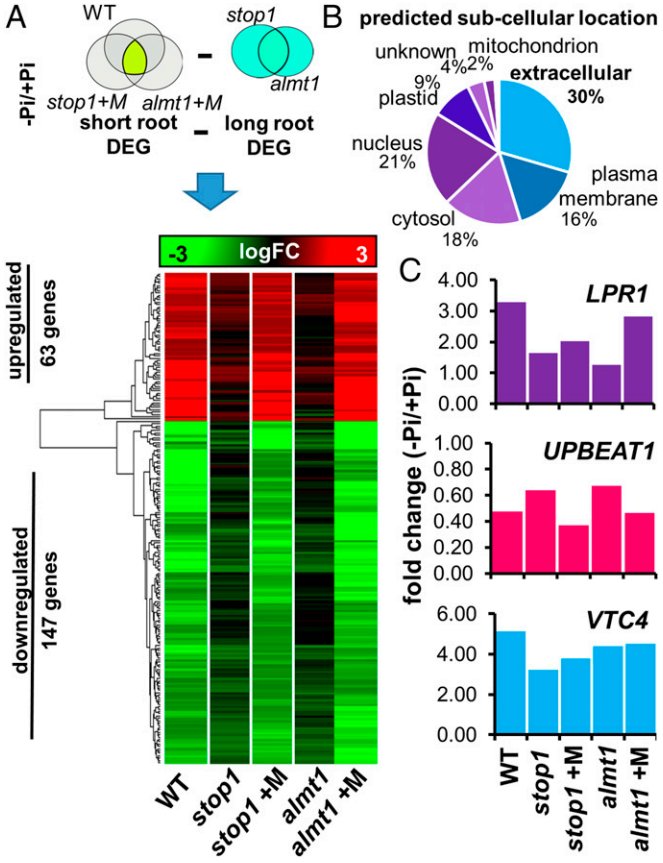

Fig. 6. Malate treatment rescues the expression of transcripts whose products are targeted to the extracellular region. (*A*) Schematic of the Venn diagram analysis of common differentially expressed genes [DEG; −1.5 > logFC(−Pi/Pi) > 1.5; FDR < 0.05] in short-root phenotypes (WT∩*stop1*∩*almt1*) minus the DEG in long-root phenotypes (*stop1*∪*almt1*) under Pi-deficiency conditions, that was performed to determine the genes whose expression is linked to short-root phenotype and is rescued by malate treatment in *stop1* and *almt1* seedlings. Heatmap of the logFC values in WT, *stop1*/+M, and *almt1*/+M of the determined gene set is presented. (*B*) Predicted subcellular location of the DEG whose expression is restored by malate treatment. (*C*) *LPR1*, *UPBEAT1*, and *VTC4* expression levels are presented in fold change (FC; FDR < 0.05) as revealed by our transcriptomic studies in the root apex of WT, *stop1*, and *almt1* seedlings under −Pi conditions and −Pi and malate treatment (*almt1*+M, *stop1*+M) conditions.

treatment on the primary root elongation of *lpr1* seedlings grown in media lacking Pi. We observed that malate treatment did not rescue the *lpr1* mutant phenotype (*SI Appendix*, Fig. S6), suggesting that the effect of malate to trigger the determinate root developmental program in response to Pi deficiency requires the presence of a functional LPR1 protein.

Because alterations in the ROS balance in the RAM of *Arabidopsis* are linked to the meristem exhaustion process observed in Pi-deprived seedlings (36) and *LPR1* is essential for the low-Pi–dependent ROS signaling that takes place in the primary root of *Arabidopsis*, we decided to analyze the transcript levels of UPBEAT1 (*UPB1*) (Fig. 6*C*): the only transcription factor known to modulate ROS balance and control the transition from cell proliferation to cell differentiation in the RAM by modulating the transcription of peroxidase genes (37). We observed that *UPB1* is down-regulated 0.48-fold in response to low Pi in the root apex of WT seedlings and that it is down-regulated to a lower degree in *stop1* [0.64 fold change (FC)] and *almt1* (0.67 FC). Malate treatment restored the down-regulation of *UPB1* in Pi-deprived *almt1* (0.46 FC) and *stop1* (0.37 FC) seedlings to WT levels (Fig. 6*C*). Because LPR1 and UPB1 seem to be involved in modulating ROS balance in the RAM and their expression is misregulated in *stop1* and *almt1*, we identified peroxidase genes that have been related to ROS homeostasis in the root (34) and analyzed their expression levels in WT, *stop1*, and *almt1* seedlings. We found that 18 peroxidase genes (*PRXS*) were transcriptionally regulated by low Pi in the root apex of WT seedlings of which 13 *PRXS* were not responsive to low Pi in *stop1* and *almt1* (Dataset S1). Interestingly, the responsiveness of 11 peroxidase genes (*PEROXIDASE52*, *AT4G08780*, *AT4G08780*, *PEROXIDASE2*, *AT5G06730*, *AT5G39580*, *PEROXIDASE37*, *AT5G15180*, *PEROXIDASE4*, *AT2G39040*, and *AT3G01190*) was rescued by malate treatment in Pi-deprived *stop1* and *almt1* seedlings (*SI Appendix*, Fig. S7). Alterations of ROS balance have been related to callose deposition in the primary root of *Arabidopsis* (20). Given that the transcription of ROS-related genes (*UPB1*, *LPR1*, and *PRXS*) is disrupted in *stop1* and *almt1* under low-Pi conditions, we analyzed the expression values of genes coding for callose synthases (*CALS*). We found that the expression of 4 genes coding for *CALS* (*CALLOSESYNTHASE7*, *CALLOSESYNTHASE9*, *GLUCANSYNTHASELIKE4*, and *GLUCANSYNTHASELIKE5*) was induced (1.1 logFC; FDR < 0.05) in the root apex of WT seedlings and that it was induced to a lesser extent (logFC < 0.6) in *stop1* and *almt1* seedlings. It was observed that malate treatment also rescued the expression of these 4 *CALS* in Pi-deprived *stop1* and *almt1* (*SI Appendix*, Fig. S7). Our results suggested that malate efflux is required for the ROS signaling cascade that has been reported to be affected in low-Pi insensitive mutants (20, 36).

Given that Fe tends to its higher oxidation state (Fe^{+3}) in natural environments and the iron uptake genes IRON REGULATED TRANSPORTER 1 (*IRT1*) and FERRIC REDUCTION OXIDASE 2 (*FRO2*) have been reported to be repressed in response to Pi-deficiency conditions (3, 5, 38) we asked whether an alternative Fe^{+3} reduction mechanism could provide Fe^{+2} to LPR1 to initiate the proposed ROS signaling cascade that is induced in the RAM in response to low Pi. An ascorbate-dependent Fe^{+2} reduction mechanism has been reported recently (29), in which VITAMINC4 (*VTC4*), a gene encoding a protein with dual myo-inositol-monophosphatase and ascorbate synthase activity (39), could play a central role. We found that *VTC4* is induced in the root apex of WT (5 FC), *almt1* (4.3 FC), and *stop1* (3.22 FC) seedlings (Fig. 6*C*). Interestingly, *VTC4* belongs to the set of genes that are direct targets of PHR1 (6), providing a potential link between local and systemic signaling in the primary root response to low Pi and the cross-talk between Fe and P in the Pi-deficiency response.

Discussion

LPR1 has been proposed to promote the accumulation of Fe in the apoplast of cells in the RAM, which in turn triggers an accumulation of callose that alters symplastic transport causing meristem differentiation (20). However, the precise mechanism by which Fe accumulates in the apoplast of RAM cells remained to be determined. Here we show that *STOP1* and *ALMT1* participate in the mechanism that triggers RAM exhaustion in response to low Pi availability by mediating the accumulation of Fe^{+3} in the apoplast of RAM cells. *STOP1* and *ALMT1* were originally described as genes responsible for the malate efflux that protects the *Arabidopsis* root from Al^{+3} toxicity (21, 22). *AtSTOP1* is constitutively expressed in *Arabidopsis*, indicating that its involvement in the Al-dependent induction of gene expression must involve posttranslational processes of modification or the direct binding of Al^{+3}. The finding that mutations in *STOP1* and *ALMT1* lead to long-root phenotypes in Pi-deprived seedlings suggests that malate excretion is also involved in the process of meristem exhaustion in response to low Pi availability. We found that *STOP1* is expressed in the RAM in a Pi-independent fashion and that *ALMT1* is expressed in the RAM but only in seedlings grown in media with low-Pi concentrations. Although the expression domains of *STOP1* and *ALMT1* do not completely overlap, we

found that the expression directed by the *ALMT1* promoter is completely dependent on an intact copy of *STOP1* (*SI Appendix*, Fig. S2). The apparent inconsistency between the role of an activator with its target gene and the differences in patterns of expression of *STOP1* and *ALMT1* could be explained by the recent report that *STOP1* mRNA is cell-to-cell mobile (40).

Pi and Fe availability have been shown to coordinately regulate RAM maintenance and primary root growth in vitro (11, 17, 20). Our results corroborate that, in *Arabidopsis* WT seedlings, Fe availability (*SI Appendix*, Fig. S8) in the medium is required for RAM exhaustion in media with a low Pi concentration and that Fe accumulation in the RAM is associated with the process of RAM exhaustion (Fig. 4). Apoplastic iron accumulation in the RAM was reported to be essential for primary root growth inhibition in response to −Pi conditions (20); however, the mechanism for iron accumulation in the root remained to be determined. We found that Fe failed to accumulate in the root apex of *stop1* and *almt1* seedlings grown in Pi-deficient media and that the treatment of *stop1* and *almt1* seedlings with malate restores both Fe accumulation in the RAM and the inhibition of primary root growth in Pi-deprived seedlings (Fig. 4). These data show that malate secretion is necessary and sufficient for iron accumulation in the RAM and to trigger cell differentiation in the RAM that is responsible for the meristem exhaustion process induced by Pi deficiency. We propose that such mechanism of iron accumulation happens in the apoplast as ALMT1 is reported to be a malate efflux protein (22) and thus, exogenous malate, which probably diffuses through the apoplast, can rescue iron accumulation in *almt1* and *stop1*. Malate supplementation was found to fully rescue the short-root phenotype of *almt1*, whereas it only partially restored primary root growth inhibition in *stop1*, suggesting that, in addition to *ALMT1*, *STOP1* regulates the expression of other genes whose activation by low Pi is required for full meristem exhaustion.

Molecular dynamic simulation of Fe^{+3} and Fe^{+2} interaction shows that malate can form large complexes with Fe^{+3} but not Fe^{+2} (*SI Appendix*, Fig. S5). These data suggest that malate promotes the accumulation of Fe^{+3} in the apoplast by forming these large molecular weight complexes, which by a still largely unknown mechanism that correlates with ROS generation (20), activate the processes required for meristem exhaustion. *lpr1* seedlings also show a long-root phenotype in low-Pi media, suggesting that the ferroxidase activity of LPR1 is required to trigger cell differentiation during the primary root meristem exhaustion process triggered by Pi deprivation. We found that the long-root phenotype of *lpr1* in low-Pi media cannot be rescued by malate treatment, suggesting that *LPR1* acts downstream of *STOP1* and *ALMT1* and that most probably is required to activate the Fe-mediated mechanism involved in the process of RAM exhaustion observed in Pi-deprived seedlings. Therefore, cell-wall–localized LPR1 ferroxidase activity, which catalyzes Fe^{+2} to Fe^{+3} conversion (20), could act synergistically with malate efflux in the accumulation of Fe^{+3} in the apoplast of RAM cells. LPR1-dependent Fe^{+3} production in the apoplast could trigger ROS production by initiating a Fe redox cycle as previously proposed (41). Either ferric-chelate reductase oxidase activity, which reduces apoplast-diffusible Fe^{+3} chelates, or effluxed ascorbate (29), could reduce the Fe^{+3} produced by LPR1 to a redox-active Fe^{+2} to complete a cycle thereby triggering root cell differentiation. Supporting this notion, *LPR1* overexpression causes ectopic Fe^{+3} and ROS generation in Pi-deprived seedlings (20). Our data suggest the existence of a *STOP1*, *ALMT1*, and *LPR1* coordinated redox mechanism that involves Fe^{+3} deposition in the apoplast of RAM cells of seedlings exposed to low Pi. *ALMT1* is transcriptionally up-regulated in a similar fashion in WT and *lpr1* mutants (33), confirming that LPR1 acts downstream of the STOP1/*ALMT1* low-Pi regulatory node.

The expression of up to 80% of the genes involved in the local response to low Pi and up to a 40% of the genes involved in the systemic response to low Pi was affected in *stop1* and *almt1* (Fig. 5*D*). The reduction in both local and systemic responses in *stop1* and *almt1*, specifically in the PHR1-direct targets, points to a cross-talk between the signaling pathways that regulates the transcriptional activation or repression of the systemic and local responses to low Pi in the root apex. However, we cannot rule out the possibility that the internal concentration of Pi could be higher in the root tip of *stop1* and *almt1* than in the WT, which could lead to a down-regulation of the systemic response, as has been suggested for plants grown in low-Pi and low-Fe conditions (17). Further experiments regarding a possible STOP1 and ALMT1 interaction directly with Pi or PHR1- or SPX-domain proteins could shed light on the existence of a coordinated response to external and internal Pi levels in the root apex. The observation that PHR1 activates the expression of the ascorbate synthase *VTC*4 under Pi-deficiency conditions together with the recent report that ascorbate efflux contributes to Fe^{+3} reduction (29), support the notion that the redox cycle that generates ROS and triggers RAM exhaustion could be controlled by both local and systemic responses to Pi starvation.

Our transcriptomic analysis revealed that *LPR1* is responsive to Pi deprivation in the root tips of WT plants (Fig. 6*C*) and that this response is significantly reduced in the root tips of *stop1* and *almt1* seedlings (Fig. 6*C*). These results suggest that a threshold level of *LPR1* is required to activate meristem exhaustion in Pi-deprived seedlings. This notion is supported by the observation that the treatment with malate that reverts the long-root phenotype of Pi-deprived *stop1* and *almt1* seedlings (Fig. 4*A*) also leads to an increase in *LPR1* transcript levels (Fig. 6*C*). Moreover, *Arabidopsis* accessions with higher *LPR1* transcription levels have shorter primary roots under low-Pi conditions (16); and we observed that, in the case of malate-treated Pi-deprived *stop1* and *almt1* seedlings, a higher *LPR1* expression in *almt1* than in *stop1* correlated with a shorter primary root in *almt1* than in *stop1* (Figs. 4*B* and 6*C*). A recent report on the interplay between the transcriptional activation of genes coding for extracellular enzymes and iron redistribution in the apoplast in response to Pi deprivation highlighted the role of the apoplast in the Pi-starvation response (33). Transcriptomic analysis of Pi-deprived *stop1* and *almt1* seedlings showed that malate treatment reactivates the low-Pi responsiveness of genes that encode extracellular proteins involved in cell-wall modification and ROS homeostasis, such as peroxidases (34). Our transcriptomic results confirm a previously reported role of apoplastic peroxidases in the Pi-starvation response (33), and highlight the role of malate secretion in the cell-wall remodeling processes potentially involved in the changes of *Arabidopsis* root system architecture induced by low Pi availability. In this context, the finding that *UPBEAT1*, a transcription factor that modulates the transition from cell proliferation to cell differentiation in the RAM by repressing peroxidase genes (37), is repressed in response to Pi-deficiency conditions and the fact its expression is altered in *stop1* and *almt1*, support the notion that ROS generation plays an important role in the root response to Pi deprivation. Further experiments regarding the specific pattern of ROS signaling in the RAM under Pi-starvation conditions are required.

A model that summarizes what is known about the local response to Pi starvation and the proposed role of *STOP1* and *ALMT1* in the root response to Pi deprivation is presented in Fig. 7. Under Pi-deficiency conditions, expression of LPR1 is enhanced by a malate-dependent mechanism, and PDR2 activity is inhibited, facilitating LPR1 mobilization from the ER to the plasma membrane (20) where LPR1 ferroxidase activity catalyzes the conversion of Fe^{+2} into Fe^{+3} in the apoplast of RAM cells (Fig. 7). The mechanisms by which LPR1 is transported from the ER to the extracellular region and how PDR2 activity is

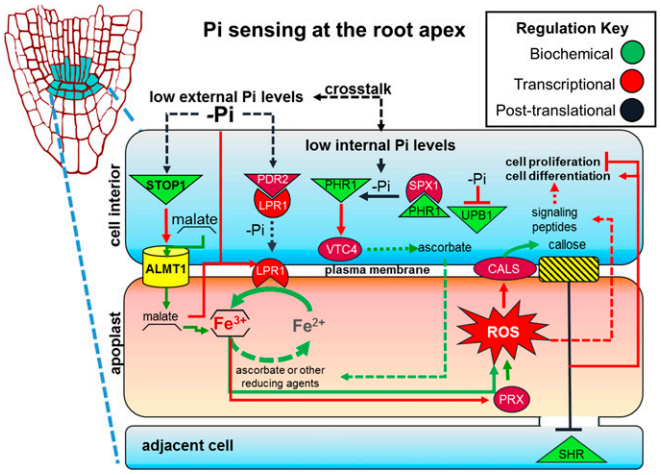

Fig. 7. *STOP1* and *ALMT1* regulate the RAM response to low-Pi conditions in *Arabidopsis*. In response to limiting Pi levels in the medium, *STOP1* induces *ALMT1* (Fig. 3), which triggers malate efflux in the root apex. Low-Pi levels also inhibit PDR2 negative regulation over LPR1 and induce, in a largely unknown mechanism, LPR1 transport to the plasma membrane. Malate contributes to the aggregation of Fe^{+3} ions in the apoplast and enhances the expression of *LPR1*, callose synthase genes (*CALS*), and peroxidase genes (*PRX*) under Pi-deficiency conditions. LPR1 and PRX activity generates reactive oxygen species (ROS), which enhance callose deposition by CALS. Callose deposition closes the symplastic channels of communication, which ultimately impairs the transport of transcription factors, such as SHR, that are essential to maintain cell proliferation and organization in the RAM. Alternative factors induced by ROS, such as signaling peptides, could also induce cell differentiation in the RAM. A cross-talk between PHR1/SPX1-dependent internal Pi sensing and external Pi sensing could be possible because of the downgrade of systemic response in low-Pi insensitive mutants. Ascorbate efflux into the apoplast or another reducing agent, could reduce Fe^{+3} to Fe^{+2} and could restart the proposed redox cycle. Ascorbate efflux could be enhanced by VTC4 activity and whose gene is induced by PHR1 when internal Pi levels are limiting. Arrows represent relationships between the components. Dotted lines represent hypothetical relations, and the regulation key illustrates the type of evidence that has been provided for that relationship.

regulated by Pi availability remain to be determined. *STOP1*, a constitutively expressed gene, up-regulates the expression of *ALMT1* in seedlings exposed to low Pi, thereby activating the excretion of malate. LPR1 ferroxidase activity in the plasma membrane of cells in the meristem and elongation zones of the primary root, locally produces Fe^{+3}, which forms large complexes with malate, leading to its accumulation. As mentioned above, we observed a cross-talk between local and systemic responses to Pi deficiency; therefore, we included the internal Pi-sensing module PHR1/SPX1 (6) in the model because it controls the majority of the systemic transcriptional responses to low Pi (5). PHR1-dependent induction of *VTC4* could enhance ascorbate efflux, which represents a potential mechanism of Fe^{+3} reduction to produce the Fe^{+2} required to complete a redox cycle that generates ROS. Expression of the *UPB1* repressor is reduced by a Fe/malate-dependent mechanism under low-Pi conditions, which enhances the transcription of peroxidase genes. Enhanced transcription of local response peroxidase genes likely triggers ROS generation in the root of Pi-deprived seedlings as previously reported (36). ROS generation triggers callose deposition as previously reported (20, 42). This notion is supported by the observation that the expression of several *CALS* genes is enhanced in the root apex of WT but not in *stop1* and *almt1* seedlings (*SI Appendix*, Fig. S7). Callose synthesis impairs symplastic transport by physically blocking plasmodesmatal pores, which reduces or inactivates the cell-to-cell movement of SHR (20). Because SHR cell-to-cell movement is required for stem cell niche maintenance, meristem exhaustion takes place in seedlings exposed to low Pi availability. However, because CLE-like peptide signaling is also required for stem cell niche maintenance in *Arabidopsis* (43), we cannot rule out that ROS or Fe^{+3} accumulation in the RAM could induce the transcription of CLE peptides that could also execute RAM exhaustion.

STOP1 controls *ALMT1* transcription and its expression is not regulated by Pi availability, suggesting that STOP1 is most likely involved in sensing external Pi levels or an environmental cue that it is linked to low-Pi levels in the medium. Because STOP1 also controls low pH and Al^{+3} toxicity responses, it emerges as a possible master regulator/sensor that orchestrates the root responses to multiple environmental stresses.

The root tip is at the forefront of nutrient sensing and acquisition; therefore, it represents the first contact of the plant with the soil solution. Previous findings have shown that the root tip plays a critical role in Pi sensing (16) and that organic acids are secreted from the roots of Pi-deprived plants to solubilize Pi and facilitate its uptake (14). We describe an organic-acid–mediated mechanism that starts in the root tip and adjusts the root developmental response to low Pi. Organic acids have also been implicated in Fe uptake (30) and protection of the root from the entrance of toxic Al^{+3} ions (22, 23). Taken all together, the evidence suggests that organic-acid exudation is a critical checkpoint in plant nutrition as these molecules do not only protect the root from the entry of toxic ions and enhance nutrient uptake, but also contribute to the modifications of root development that increase the soil-exploration ability of the plant to enhance nutrient uptake. Biotechnological approaches, like the overexpression of *ALMT1* or *STOP1*, could be coupled with the metabolic engineering of carbon metabolism in plants to optimize nutrient uptake in an agricultural environment.

Materials and Methods

Plant Material. *A. thaliana* Col-0 accession (CS70000) was used in this work. *stop1*-SALK_114108 (N614108), *almt1*-SALK_009629 (N509629), and *lpr1* (N516297) lines were provided by the Nottingham *Arabidopsis* Stock Center (NASC).

Growing Conditions. Seeds were surface sterilized and sown in 1% agar, 0.1× Murashige and Skoog (MS) medium as described in ref. 10. A total of 1 mM KH_2PO_4 (high Pi; +Pi) or 5 μM KH_2PO_4 (low Pi; −Pi) Pi concentrations were used. A total of 1% (wt/vol) sucrose and 3.5 mM MES was added. Fe-free medium was prepared as described (15), and 100 μM ferrozine (Sigma, 82950) was added to reduce agar Fe availability. Malate and citrate (Sigma, M1000 and Sigma, C0759, respectively) were added to medium before sterilization. Seedlings were grown in a Percival chamber at 22 °C, under 16/8 h photoperiod with >200 $\mu mol \cdot m^{-2} \cdot s^{-1}$ luminous intensity.

Gene Mapping. Plant mapping populations were built crossing *lpi5* and *lpi6* homozygous lines vs. Col-0 (CS70000), respectively, according to the Mutmap protocol (44). Heterozygous F1 plants were self-fertilized for seed propagation. The F2 segregating individuals were rescreened for WT (short root) and mutant (long root) phenotypes, respectively, for each of the two crosses. Then, DNA was extracted from 100 plants for each phenotype, pooled, and sequenced using Illumina Miseq technology (paired end, 250 base pair reads in length). Reads obtained were processed with fastQC and Trimmomatic (45) to improve their quality. Only paired-end reads were considered. Reads were mapped to the Col-0 reference genome (TAIR10) using BWA (46) and SAMtools (47). To identify and to evaluate specific variants related to the mutant phenotype (long root), a pipeline using GATK (https://software.broadinstitute.org/gatk/), VCFtools (48), SNPeff, and SNPshif (49) was implemented. IGV was used to visualize variants (50).

Histochemical Iron Staining. Perls iron staining and DAB intensification were carried out as described in ref. 20 and analyzed using Nomarski optics on a Leica DMR microscope. To improve the resolution of the picture, optical sections of ∼40 μM were taken with a 100× objective and assembled into photographic reconstructions using Adobe Photoshop. No other manipulation of the images was used.

RNA-Seq High-Throughput Sequencing and Data Analysis. High-throughput sequencing and data analysis were carried out as described (51).

qRT-PCR. Total RNA was isolated using TRIzol reagent (Invitrogen) according to the manufacturer's instructions. Real-time PCR was performed with an Applied Biosystems 7500 real-time PCR system using SYBR Green detection chemistry (Applied Biosystems) and gene-specific primers. The relative expression levels were computed by the Ct method of relative quantification. Oligonucleotide primer sequences are available upon request.

A more detailed version of materials and methods is included in *SI Appendix, SI Materials and Methods*.

ACKNOWLEDGMENTS. We thank G. S. Gillmor for his advice on EMS seed mutagenesis and L. F. García-Ortega and O. Martínez for help in calculating the dispersion values for the normalization of transcriptomic data expression. J.M.-M. is indebted to Consejo Nacional de Ciencia y Tecnología (CONACyT) for a PhD fellowship. J.O.O.-R. is indebted to CONACyT for an MSc fellowship. This research was supported by CONACyT Ciencia Básica Grant 252039 (to L.H.-E.) and by Howard Hughes Medical Institute Grant 4367 (to L.H.-E.).

1. Marschner H (2011) *Marschner's Mineral Nutrition of Higher Plants* (Elsevier Science, Amsterdam, The Netherlands).
2. Wu P, et al. (2003) Phosphate starvation triggers distinct alterations of genome expression in Arabidopsis roots and leaves. *Plant Physiol* 132:1260–1271.
3. Misson J, et al. (2005) A genome-wide transcriptional analysis using *Arabidopsis thaliana* Affymetrix gene chips determined plant responses to phosphate deprivation. *Proc Natl Acad Sci USA* 102:11934–11939.
4. Morcuende R, et al. (2007) Genome-wide reprogramming of metabolism and regulatory networks of Arabidopsis in response to phosphorus. *Plant Cell Environ* 30:85–112.
5. Thibaud MC, et al. (2010) Dissection of local and systemic transcriptional responses to phosphate starvation in Arabidopsis. *Plant J* 64:775–789.
6. Bustos R, et al. (2010) A central regulatory system largely controls transcriptional activation and repression responses to phosphate starvation in Arabidopsis. *PLoS Genet* 6:e1001102.
7. Hoffland E, Van Den Boogaard R, Nelemans J, Findenegg G (1992) Biosynthesis and root exudation of citric and malic acids in phosphate-starved rape plants. *New Phytol* 122:675–680.
8. Cruz-Ramírez A, Oropeza-Aburto A, Razo-Hernández F, Ramírez-Chávez E, Herrera-Estrella L (2006) Phospholipase DZ2 plays an important role in extraplastidic galactolipid biosynthesis and phosphate recycling in Arabidopsis roots. *Proc Natl Acad Sci USA* 103:6765–6770.
9. Bates TR, Lynch JP (1996) Stimulation of root hair elongation in *Arabidopsis thaliana* by low phosphorus availability. *Plant Cell Environ* 19:529–538.
10. López-Bucio J, et al. (2002) Phosphate availability alters architecture and causes changes in hormone sensitivity in the Arabidopsis root system. *Plant Physiol* 129:244–256.
11. Sánchez-Calderón L, et al. (2005) Phosphate starvation induces a determinate developmental program in the roots of Arabidopsis thaliana. *Plant Cell Physiol* 46:174–184.
12. Péret B, Clément M, Nussaume L, Desnos T (2011) Root developmental adaptation to phosphate starvation: better safe than sorry. *Trends Plant Sci* 16:442–450.
13. Rubio V, et al. (2001) A conserved MYB transcription factor involved in phosphate starvation signaling both in vascular plants and in unicellular algae. *Genes Dev* 15: 2122–2133.
14. Raghothama KG (1999) Phosphate acquisition. *Annu Rev Plant Physiol Plant Mol Biol* 50:665–693.
15. Sánchez-Calderón L, et al. (2006) Characterization of low phosphorus insensitive mutants reveals a crosstalk between low phosphorus-induced determinate root development and the activation of genes involved in the adaptation of Arabidopsis to phosphorus deficiency. *Plant Physiol* 140:879–889.
16. Svistoonoff S, et al. (2007) Root tip contact with low-phosphate media reprograms plant root architecture. *Nat Genet* 39:792–796.
17. Ward JT, Lahner B, Yakubova E, Salt DE, Raghothama KG (2008) The effect of iron on the primary root elongation of Arabidopsis during phosphate deficiency. *Plant Physiol* 147:1181–1191.
18. Ticconi CA, Delatorre CA, Lahner B, Salt DE, Abel S (2004) Arabidopsis pdr2 reveals a phosphate-sensitive checkpoint in root development. *Plant J* 37:801–814.
19. Ticconi CA, et al. (2009) ER-resident proteins PDR2 and LPR1 mediate the developmental response of root meristems to phosphate availability. *Proc Natl Acad Sci USA* 106:14174–14179.
20. Müller J, et al. (2015) Iron-dependent callose deposition adjusts root meristem maintenance to phosphate availability. *Dev Cell* 33:216–230.
21. Iuchi S, et al. (2007) Zinc finger protein STOP1 is critical for proton tolerance in Arabidopsis and coregulates a key gene in aluminum tolerance. *Proc Natl Acad Sci USA* 104:9900–9905.
22. Hoekenga OA, et al. (2006) AtALMT1, which encodes a malate transporter, is identified as one of several genes critical for aluminum tolerance in Arabidopsis. *Proc Natl Acad Sci USA* 103:9738–9743.
23. Kobayashi Y, et al. (2007) Characterization of AtALMT1 expression in aluminum-inducible malate release and its role for rhizotoxic stress tolerance in Arabidopsis. *Plant Physiol* 145:843–852.
24. Colón-Carmona A, You R, Haimovitch-Gal T, Doerner P (1999) Technical advance: Spatio-temporal analysis of mitotic activity with a labile cyclin-GUS fusion protein. *Plant J* 20:503–508.
25. Sabatini S, et al. (1999) An auxin-dependent distal organizer of pattern and polarity in the Arabidopsis root. *Cell* 99:463–472.
26. Sawaki Y, et al. (2009) STOP1 regulates multiple genes that protect arabidopsis from proton and aluminum toxicities. *Plant Physiol* 150:281–294.
27. Tokizawa M, et al. (2015) SENSITIVE TO PROTON RHIZOTOXICITY1, CALMODULIN BINDING TRANSCRIPTION ACTIVATOR2, and other transcription factors are involved in ALUMINUM-ACTIVATED MALATE TRANSPORTER1 expression. *Plant Physiol* 167:991–1003.
28. Jones DL (1998) Organic acids in the rhizosphere: A critical review. *Plant Soil* 205:25–44.
29. Grillet L, et al. (2014) Ascorbate efflux as a new strategy for iron reduction and transport in plants. *J Biol Chem* 289:2515–2525.
30. Rellán-Alvarez R, et al. (2010) Identification of a tri-iron(III), tri-citrate complex in the xylem sap of iron-deficient tomato resupplied with iron: New insights into plant iron long-distance transport. *Plant Cell Physiol* 51:91–102.
31. Ziegler J, et al. (2016) Non-targeted profiling of semi-polar metabolites in Arabidopsis root exudates uncovers a role for coumarin secretion and lignification during the local response to phosphate limitation. *J Exp Bot* 67:1421–1432.
32. Puga MI, et al. (2014) SPX1 is a phosphate-dependent inhibitor of Phosphate Starvation Response 1 in Arabidopsis. *Proc Natl Acad Sci USA* 111:14947–14952.
33. Hoehenwarter W, et al. (2016) Comparative expression profiling reveals a role of the root apoplast in local phosphate response. *BMC Plant Biol* 16:106.
34. Francoz E, et al. (2015) Roles of cell wall peroxidases in plant development. *Phytochemistry* 112:15–21.
35. Tanz SK, et al. (2013) SUBA3: A database for integrating experimentation and prediction to define the SUBcellular location of proteins in Arabidopsis. *Nucleic Acids Res* 41:D1185–D1191.
36. Chacón-López A, Ibarra-Laclette E, Sánchez-Calderón L, Gutiérrez-Alanis D, Herrera-Estrella L (2011) Global expression pattern comparison between low phosphorus insensitive 4 and WT Arabidopsis reveals an important role of reactive oxygen species and jasmonic acid in the root tip response to phosphate starvation. *Plant Signal Behav* 6:382–392.
37. Tsukagoshi H, Busch W, Benfey PN (2010) Transcriptional regulation of ROS controls transition from proliferation to differentiation in the root. *Cell* 143:606–616.
38. Li W, Lan P (2015) Genome-wide analysis of overlapping genes regulated by iron deficiency and phosphate starvation reveals new interactions in Arabidopsis roots. *BMC Res Notes* 8:555.
39. Torabinejad J, Donahue JL, Gunesekera BN, Allen-Daniels MJ, Gillaspy GE (2009) VTC4 is a bifunctional enzyme that affects myoinositol and ascorbate biosynthesis in plants. *Plant Physiol* 150:951–961.
40. Thieme CJ, et al. (2015) Endogenous Arabidopsis messenger RNAs transported to distant tissues. *Nat Plants* 1:15025.
41. Kosman DJ (2010) Redox cycling in iron uptake, efflux, and trafficking. *J Biol Chem* 285:26729–26735.
42. Luna E, et al. (2011) Callose deposition: A multifaceted plant defense response. *Mol Plant Microbe Interact* 24:183–193.
43. Matsuzaki Y, Ogawa-Ohnishi M, Mori A, Matsubayashi Y (2010) Secreted peptide signals required for maintenance of root stem cell niche in Arabidopsis. *Science* 329: 1065–1067.
44. Abe A, et al. (2012) Genome sequencing reveals agronomically important loci in rice using MutMap. *Nat Biotechnol* 30:174–178.
45. Bolger AM, Lohse M, Usadel B (2014) Trimmomatic: A flexible trimmer for Illumina sequence data. *Bioinformatics* 30:2114–2120.
46. Li H, Durbin R (2009) Fast and accurate short read alignment with Burrows-Wheeler transform. *Bioinformatics* 25:1754–1760.
47. Li H, et al.; 1000 Genome Project Data Processing Subgroup (2009) The Sequence Alignment/Map format and SAMtools. *Bioinformatics* 25:2078–2079.
48. Danecek P, et al.; 1000 Genomes Project Analysis Group (2011) The variant call format and VCFtools. *Bioinformatics* 27:2156–2158.
49. Cingolani P, et al. (2012) A program for annotating and predicting the effects of single nucleotide polymorphisms, SnpEff: SNPs in the genome of Drosophila melanogaster strain w1118; iso-2; iso-3. *Fly (Austin)* 6:80–92.
50. Robinson JT, et al. (2011) Integrative genomics viewer. *Nat Biotechnol* 29:24–26.
51. Yong-Villalobos L, et al. (2015) Methylome analysis reveals an important role for epigenetic changes in the regulation of the Arabidopsis response to phosphate starvation. *Proc Natl Acad Sci USA* 112:E7293–E7302.